Interplay of Orbital Tuning and Linker Location in Controlling Electronic Communication in Porphyrin Arrays

Sung Ik Yang,[†] Jyoti Seth,[‡] Thiagarajan Balasubramanian,[§] Dongho Kim,[†,||] Jonathan S. Lindsey,*[,§] Dewey Holten,*[,†] and David F. Bocian*[,‡]

Contribution from the Departments of Chemistry, North Carolina State University, Raleigh, North Carolina 27695-8204, Washington University, St. Louis, Missouri 63130-4899, and University of California, Riverside, California 92521-0403

Received December 7, 1998

Abstract: The β-diphenylethyne-linked porphyrin dimers ZnFbU-β (nonlinking *meso*-mesityl substituents) and F_{30}ZnFbU-β (nonlinking *meso*-pentafluorophenyl substituents) and their bis-Zn analogues have been examined by static spectroscopic (absorption, fluorescence, electron paramagnetic resonance), time-resolved spectroscopic (absorption, fluorescence), and electrochemical (cyclic and square-wave voltammetry, coulometry) methods. The β-linked dimers were examined to test the hypothesis that the nature of the porphyrin HOMO (a_{1u} versus a_{2u}) in concert with the position of the linker (β-pyrrole or *meso* carbon) mediates electronic communication (excited-state energy transfer, ground-state hole-hopping). The major findings are as follows: (1) The rate of energy transfer is $(56\ ps)^{-1}$ for ZnFbU-β and $(24\ ps)^{-1}$ for F_{30}ZnFbU-β. (2) The rate of hole/electron hopping in the monooxidized bis-Zn complex $[F_{30}Zn_2U\text{-}\beta]^+$ is in the fast-exchange limit and is at least comparable to that for $[Zn_2U\text{-}\beta]^+$. These findings indicate that the presence of pentafluorophenyl groups causes *enhancement* of electronic communication in the β-linked dimers but *attenuation* in the *meso*-linked dimers. These opposite effects in the β- versus *meso*-linked dimers are explained by the fact that both pentafluorophenyl-substituted dimers have a_{1u} HOMOs, which exhibit significant β-pyrrole electron density, whereas both mesityl-substituted dimers have a_{2u} HOMOs, which exhibit large *meso*-carbon density. Thus, the combination of an a_{1u} HOMO with a β-linker or an a_{2u} HOMO with a *meso* linker results in optimal electronic communication. Collectively, these results demonstrate that the nature of the frontier orbitals and position of connection of a covalent linker (in addition to distance, orientation, and energetics) must be considered in the design architecture of molecular photonic devices.

I. Introduction

The rational design of molecular devices that support efficient photoinduced energy transfer requires a fundamental knowledge of the mechanisms of electronic communication. As part of a program in the design of porphyrin-based molecular photonic devices, our groups have prepared and studied a variety of porphyrin dimers with the aim of probing pairwise electronic interactions between the porphyrin constituents.[1−8] One prototypical class of dimers has a diarylethyne linker attached to the porphyrin *meso* positions, with the remaining nonlinking *meso* positions substituted with solubilizing aryl groups. For this general class of dimers, we have shown that excited-state energy transfer from a metalloporphyrin (Zn/Mg/Cd) to a free base (Fb) porphyrin proceeds primarily via a through-bond (TB) process mediated by the diarylethyne linker. The diarylethyne linker also mediates ground-state hole/electron hopping in the π-cation radicals of the bis-metallo analogues of the dimers.

Recently, we found that the rate of excited-state energy transfer (and ground-state hole/electron hopping) in the diarylethyne-linked porphyrin dimers is significantly influenced by the electron-withdrawing/-releasing properties of the nonlinking aryl substituents.[5] In particular, the energy-transfer rate in ZnFbU is $(24\ ps)^{-1}$, while the rate in the pentafluorophenyl-substituted analogue F_{30}ZnFbU is $(240\ ps)^{-1}$ (Figure 1). The 10-fold slower rate in the latter dimer is attributed primarily to a switch in the nature of the highest occupied molecular orbital (HOMO) on each porphyrin from a_{2u} in ZnFbU to a_{1u} in F_{30}-ZnFbU (although the electron-withdrawing effects of the pentafluorophenyl groups may also contribute to changes in the electron distribution in the HOMO and in the lowest occupied molecular orbitals (LUMOs)). The switch of the HOMO due to the presence of the electron-withdrawing pentafluorophenyl groups also results in much slower (at least 10-fold) ground-state hole/electron hopping in $[F_{30}Zn_2U]^+$ versus $[Zn_2U]^+$.[5]

[†] Washington University.
[‡] University of California.
[§] North Carolina State University.
[||] Permanent address: Spectroscopy Lab, Korea Research Institute of Standards and Science, P.O. Box 102, Yusong, Taejon 305-600, Korea.

(1) Wagner, R. W.; Lindsey, J. S.; Seth, J.; Palaniappan, V.; Bocian, D. F. *J. Am. Chem. Soc.* **1996**, *118*, 3996−3997.
(2) Seth, J.; Palaniappan, V.; Wagner, R. W.; Johnson, T. E.; Lindsey, J. S.; Bocian, D. F. *J. Am. Chem. Soc.* **1996**, *118*, 11194−11207.
(3) Hsiao, J.-S.; Krueger, B. P.; Wagner, R. W.; Delaney, J. K.; Mauzerall, D. C.; Fleming, G. R.; Lindsey, J. S.; Bocian, D. F.; Donohoe, R. J. *J. Am. Chem. Soc.* **1996**, *118*, 11181−11193.
(4) Li, F.; Gentemann, S.; Kalsbeck, W. A.; Seth, J.; Lindsey, J. S.; Holten, D.; Bocian, D. F. *J. Mater. Chem.* **1997**, *7*, 1245−1262.
(5) Strachan, J. P.; Gentemann, S.; Seth, J.; Kalsbeck, W. A.; Lindsey, J. S.; Holten, D.; Bocian, D. F. *J. Am. Chem. Soc.* **1997**, *119*, 11191−11201.
(6) Strachan, J. P.; Gentemann, S.; Seth, J.; Kalsbeck, W. A.; Lindsey, J. S.; Holten, D.; Bocian, D. F. *Inorg. Chem.* **1998**, *37*, 1191−1201.
(7) Yang, S. I.; Lammi, R. K.; Seth, J.; Riggs, J. A.; Arai, T.; Kim, D.; Bocian, D. F.; Holten, D.; Lindsey, J. S. *J. Phys. Chem. B* **1998**, *102*, 9426−9436.
(8) Hascoat, P.; Yang, S. I.; Seth, J.; Lindsey, J. S.; Bocian, D. F.; Holten, D. Manuscript in preparation.

10.1021/ja9842060 CCC: $18.00
Published on Web 04/09/1999

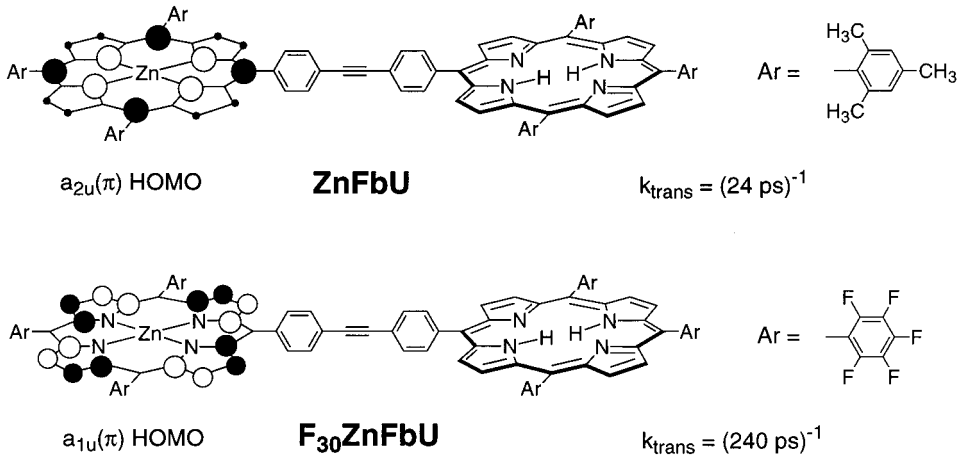

Figure 1. Structures, schematic electron-density distributions, and photoinduced energy-transfer rates in the *meso*-linked arrays studied previously. Note that higher level molecular orbital calculations predict that the a_{2u} orbital has a small amount of electron density at the β-carbons.

The changes in electronic communication due to electron-withdrawing/-releasing effects of substituents in the diarylethyne-linked porphyrin dimers can be rationalized via consideration of the attributes of the porphyrin frontier molecular orbitals. The a_{2u} and a_{1u} orbitals of both metalloporphyrins and Fb porphyrins are in close energetic proximity.[9,10] These orbitals have quantitatively different electron-density distributions. The a_{2u} orbital has electron density at the *meso* positions and the central nitrogens, whereas the a_{1u} orbital has nodes at these positions but exhibits considerable electron density at the pyrrole carbons (Figure 1). The energy spacing and ordering of the a_{2u} and a_{1u} orbitals are particularly sensitive to the electron-withdrawing/-releasing effects of the substituent groups that are positioned at the periphery of the macrocycle. Strong electron-withdrawing groups, such as the pentafluorophenyl groups of F_{30}ZnFbU (and $F_{30}Zn_2U$), stabilize the a_{2u} orbital to such an extent relative to the a_{1u} orbital that the former orbital drops below the latter. This orbital-reversal effect in turn modulates the electron density at the position of linker attachment. In addition, the overall electron density in the macrocycle is reduced and shifted onto the pentafluorophenyl rings. This latter effect also stabilizes the two e_g* LUMOS, but by comparable amounts because they have comparable electron density at the *meso* positions (in both the metalloporphyrins and Fb porphyrins[9,10]). The magnitude of the linker-mediated electronic coupling between the porphyrins in an array depends on the electron density at the position to which the linker is attached to each macrocycle. Thus, the reversed energy ordering of the a_{1u} and a_{2u} orbitals that accompanies exchange of the nonlinking mesityl rings with pentafluorophenyl groups changes the relative contributions of the two orbitals to the linker-mediated interporphyrin electronic interactions. In particular, the electronic communication in a *meso*-linked dimer with an a_{1u} HOMO (such as F_{30}ZnFbU) is attenuated compared with a *meso*-linked dimer with an a_{2u} HOMO (such as ZnFbU). As a consequence, F_{30}-ZnFbU exhibits a slower rate of excited-state energy transfer than does ZnFbU, and $[F_{30}Zn_2U]^+$ exhibits a slower rate of ground-state hole/electron hopping than does $[Zn_2U]^+$.

The hypothesis that the characteristics of the frontier molecular orbitals (spacing, ordering, and electron-density distributions) affect the rate of TB electronic communication, if generally true, has important implications for the design of porphyrin-based molecular devices. To date, our evidence for the effects of orbital characteristics on electronic communication stems entirely from studies of porphyrin dimers joined at the *meso* positions (Figure 1). To test the generality of these effects, we sought to examine the electronic communication in analogous dimers in which each monomeric unit of ZnFbU and F_{30}-ZnFbU has the diphenylethyne linker switched from a *meso* position to a β-pyrrole position while otherwise remaining the same. This requirement led to the structures shown in Figure 2 (designated ZnFbU-β and F_{30}ZnFbU-β). The presence of electron-withdrawing pentafluorophenyl groups in the β-linked dimers should affect excited-state energy transfer and ground-state hole/electron hopping in a manner opposite that in the *meso*-linked arrays. This hypothesis is tested herein, where we report a detailed spectroscopic study of the β-linked dimers shown in Figure 2. The studies of these dimers, in conjunction with our earlier work on the *meso*-linked analogues, reveal the importance of the interplay of orbital characteristics and linker location in controlling electronic communication in porphyrin-based arrays.

II. Results

A. Synthesis. Each porphyrin monomer used to construct the β-linked dimers has one β-substituent, no substituent at the flanking *meso* position, and three identical groups at the nonflanking *meso* positions (Figure 2). Each porphyrin in the series of β-linked or *meso*-linked dimers thus has four aryl substituents, comprised of the linker and three nonlinking *meso* substituents. The absence of a substituent at the *meso* position flanking the β-pyrrole linker is a critical feature designed to avoid unwanted steric interactions. The synthesis of the β-linked dimers could not rely on established methods for preparing porphyrins with flanking *meso* and β-substituents but required the development of new approaches for synthesizing the monomeric porphyrin building blocks. The synthesis of the monomers and dimers is described elsewhere.[11]

B. Physical Properties of the Neutral Complexes. (1) Absorption Spectra. Visible-region electronic ground-state absorption spectra of the β-linked ZnFb dimers (ZnFbU-β, F_{30}-ZnFbU-β) and selected β-substituted monomeric reference compounds (FbU-β, F_{15}FbU-β, ZnU-β, F_{15}ZnU-β) are shown in Figure 3. For comparison, visible-region spectra of the *meso*-substituted analogues (e.g., ZnFbU and F_{30}ZnFbU) that we studied previously[3−5,12] are shown in Figure 4. Absorption

(9) Gouterman, M. In *The Porphyrins*; Dolphin, D., Ed.; Academic Press: New York, 1978; Vol. 3, pp 1−165.

(10) Spellane, J. P.; Gouterman, M.; Antipas, A.; Kim, S.; Liu, Y. C. *Inorg. Chem.* **1980**, *19*, 386−391.

(11) Balasubramanian, T.; Lindsey, J. S. *Tetrahedron.* In press.

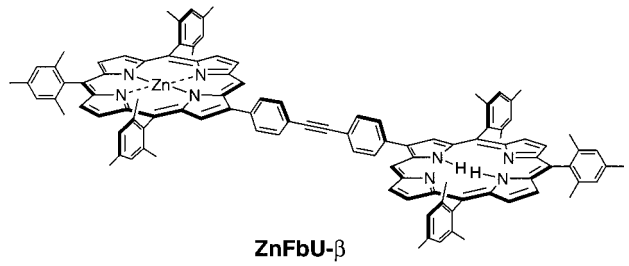

ZnFbU-β

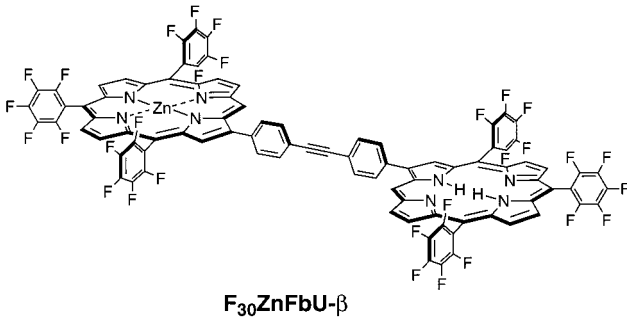

F_{30}ZnFbU-β

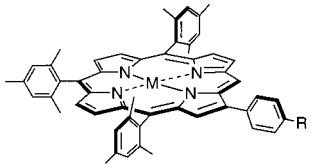

M	R	Compd
H,H	I	**FbI-β**
Zn	I	**ZnI-β**
H,H	CCTMS	**FbU-β**
Zn	CCTMS	**ZnU-β**
Zn	CCH	**ZnU'-β**

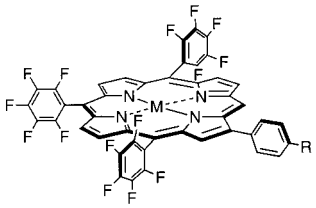

M	R	Compd
H,H	I	**F_{15}FbI-β**
H,H	CCTBDMS	**F_{15}FbU-β**
Zn	CCTBDMS	**F_{15}ZnU-β**

Figure 2. Structures of the β-linked dimers studied here and various monomeric building blocks. The dimers are displayed in the *transoid* conformation (CCTMS = trimethylsilylethynyl; CCTBDMS = *tert*-butyldimethylsilylethynyl).

maxima and intensity ratios for both classes of compounds are given in the Supporting Information. The absorption spectra of the β-substituted complexes exhibit the same general characteristics as the *meso*-substituted compounds and other porphyrins. In particular, the spectra of the β-substituted porphyrins have a strong near-UV Soret (B) band (not shown) and a series of weaker visible (Q) bands (Figure 3). For the Fb porphyrins, the four Q-bands $Q_y(1,0)$, $Q_y(0,0)$, $Q_x(1,0)$, and $Q_x(0,0)$ lie in the vicinity of 510, 545, 585, and 640 nm, respectively. For the Zn porphyrins, the two Q-bands Q(1,0) and Q(0,0) occur near 545 and 580 nm, respectively.

Several noteworthy comparisons can be made concerning the absorption characteristics of the β- and *meso*-substituted complexes. (1) The spectra of the β-linked dimers (in both the Q and B regions) are essentially given by the sum of the spectra

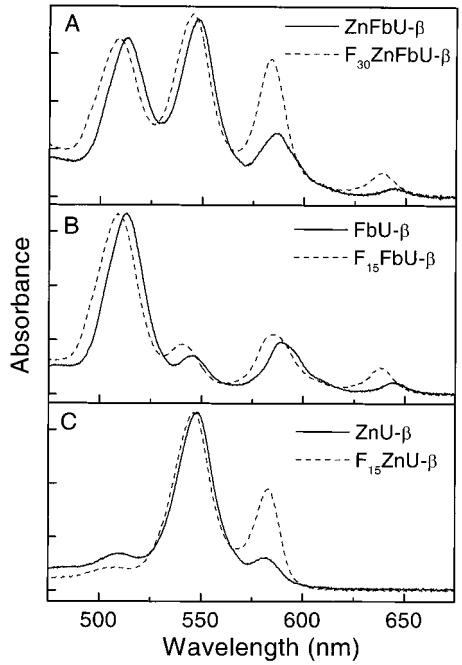

Figure 3. Electronic ground-state absorption spectra (in toluene at room temperature) in the Q-band region for the β-substituted dimers and monomeric reference compounds. The data were taken in toluene at room temperature.

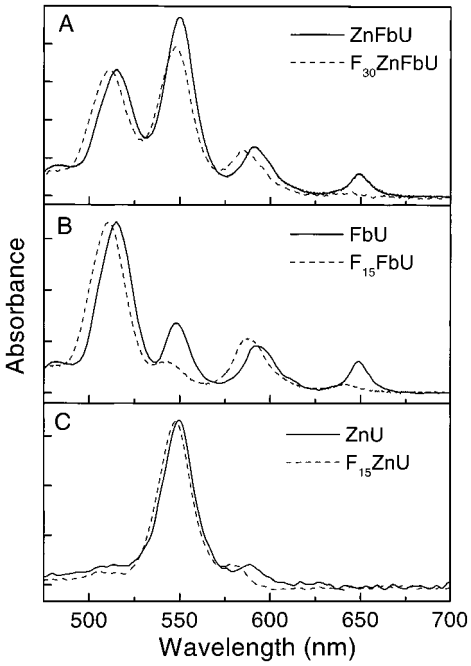

Figure 4. Electronic ground-state absorption spectra (in toluene at room temperature) in the Q-band region for the *meso*-substituted dimers and monomeric reference compounds. The data were taken from refs 2−5 and 12.

of the individual constituents. This finding is indicative of relatively weak interactions between the porphyrin constituents of the β-linked dimers, as is also the case for the *meso*-linked analogues.[2−5] (2) The Q-band maxima of the β-substituted complexes are typically slightly blue-shifted from those of their *meso*-substituted counterparts, while the Soret maxima are affected little if at all.[13] (3) The presence of pentafluorophenyl groups affects the wavelength maxima of the β-substituted complexes in a manner similar to that found previously for the *meso*-substituted complexes.[5,12] In particular, the presence of

(12) Yang, S. I.; Seth, J.; Strachan, J. P.; Gentemann, S.; Kim, D.; Holten, D.; Lindsey, J. S.; Bocian, D. F. *J. Porphyrins Phthalocyanines* **1999**, *3*, 117−147.

(13) The small blue shifts in the optical bands are consistent with the removal of one non-hydrogen *meso* substituent and the addition of one non-hydrogen β-pyrrole substituent in the β- versus *meso*-substituted compounds (compare Figures 1 and 2). The extreme example of such changes is that the absorption spectra of complexes bearing only β-pyrrole substituents such as Fb octaethylporphyrin are blue-shifted from complexes containing only *meso* substituents such as Fb tetraphenylporphyrin or its tetraalkylporphyrin analogues.

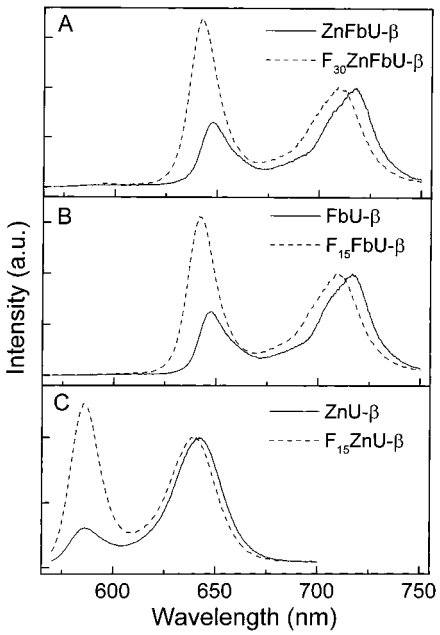

Figure 5. Fluorescence spectra (in toluene at room temperature) for selected β-substituted dimers and monomeric reference compounds.

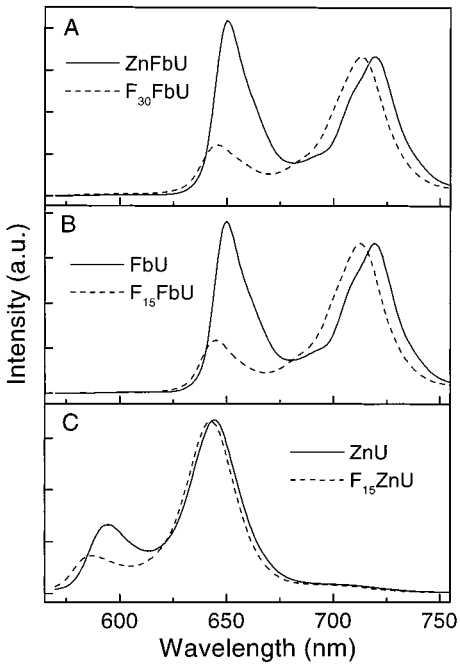

Figure 6. Fluorescence spectra (in toluene at room temperature) for selected *meso*-substituted dimers and monomeric reference compounds. The data were taken from refs 2−5 and 12.

the strongly electron-withdrawing pentafluorophenyl groups causes a blue shift of the absorption maxima, with the effects being somewhat larger for the Fb than Zn porphyrins. (4) The Q-band intensity ratios differ for analogous members of the two substitution types (e.g. FbU-β in Figure 3B versus FbU in Figure 4B). (5) The effects of the pentafluorophenyl groups on the Q-band intensity ratios are notably different for analogous β- versus *meso*-substituted compounds. For example, the $Q_x(0,0)$ transition (640−650 nm) is stronger for F_{30}ZnFbU-β than for ZnFbU-β, while the opposite is true for F_{30}ZnFbU versus ZnFbU.

The variations in the Q-band intensity ratios noted in points 4 and 5 above arise largely from modulation of the oscillator strengths of the origin transitions, namely Q(0,0) for the Zn porphyrins and $Q_x(0,0)$ plus $Q_y(0,0)$ for the Fb porphyrins. To make this observation clear, the spectra in each panel in Figures 3 and 4 are normalized to the Q(1,0) transition for the Zn porphyrins and the $Q_x(1,0)$ transition for the Fb porphyrins (and the ZnFb dimers). These satellite bands have relatively constant extinction coefficients because their strengths are derived predominantly via vibronic borrowing from the intense Soret transition.[9] The observed intensity variations are significant because, according to the four-orbital model, the strength of the $S_0 \rightarrow Q$ transition (as reflected largely in the Q(0,0) intensity) depends critically on the relative energies (spacing, not ordering) of the porphyrin a_{1u} and a_{2u} orbitals.[9,10] In particular, the Q(0,0) intensity decreases as the a_{1u} and a_{2u} orbitals move closer together in energy. Thus, inspection of the intensities of the longest wavelength Q-bands in Figures 3 and 4 indicates the following. (1) The a_{1u} and a_{2u} orbitals lie energetically farther apart in F_{15}FbU-β than in FbU-β, while the opposite is true for F_{15}FbU versus FbU. (2) The two orbitals have a larger spacing in F_{15}ZnU-β than in ZnU-β, whereas they have comparable (and small) spacings in F_{15}ZnU and ZnU. The orbital ordering switches but the spacing remains about the same for the last two *meso*-linked Zn monomers (as determined from our study of an extensive series of halogenated porphyrin building blocks[12]). Finally, the overall similarities of the peak positions among the spectra of the *meso*- and β-substituted complexes indicates that these molecules have comparable gaps between the energy centroid of the a_{1u}/a_{2u} orbitals and the energy of the e_g* orbitals.

(2) Fluorescence Spectra. Emission spectra of the β-linked dimers and selected β-substituted monomers are shown in Figure 5. For comparison, spectra of the analogous *meso*-substituted complexes studied previously are shown in Figure 6. The emission wavelengths and intensity ratios for both classes of complexes are given in the Supporting Information. The emission spectra of all of the compounds are dominated by two main features, namely the Q(0,0) and Q(0,1) bands. The Q(0,0) and Q(0,1) emission bands occur near 640−650 and 710−720 nm, respectively, for the Fb constituents and near 585−595 and 640−645 nm, respectively, for the Zn components.

Before making comparisons among the emission spectra of the various complexes, it is important to note a significant general aspect of the emission from ZnFbU-β and F_{30}ZnFbU-β. In particular, the emission from both ZnFb complexes originates nearly exclusively from the Fb component, irrespective of whether the Fb or Zn porphyrin is photoexcited. For example, illumination of ZnFbU-β near 550 nm, where the Zn porphyrin preferentially absorbs, primarily affords a Fb-porphyrin emission spectrum with no noticeable emission from the Zn component (compare solid spectra in parts A−C of Figure 5). The same is true of F_{30}ZnFbU-β (dashed spectra in Figure 5). Thus, the observed emission spectra of both ZnFbU-β and F_{30}ZnFbU-β are consistent with a high yield (well over 90%) of energy transfer from the photoexcited Zn porphyrin (Zn*) to the Fb porphyrin. These results are analogous to those we have reported previously for the corresponding *meso*-linked complexes (ZnFbU and F_{30}ZnFbU), as represented by the emission spectra shown in Figure 6.[5,12]

Comparison of the $S_1 \rightarrow S_0$ emission spectra of the various β- and *meso*-substituted complexes reveals trends similar to those described above for the $S_0 \rightarrow S_1$ absorption spectra. Notable aspects of the emission data are as follows. (1) The fluorescence bands of the β-linked dimers and β-substituted monomers are generally slightly blue-shifted from the positions

Table 1. Photophysical Data for β-Linked Dimers and Reference Compounds[a]

	Φ_f		τ (ns)[b]		
compd	Zn	Fb	Zn	Fb	$(k_{rad})^{-1}$ (ns)[c]
			Dimers		
ZnFbU-β	<0.001	0.066	0.055	13.5	204
F_{30}ZnFbU-β	<0.001	0.093	0.024	11.9	108
Zn_2U-β	0.040		2.4		60
$F_{30}Zn_2$U-β	0.041		1.7		41
ZnFbU	<0.002[d]	0.13[d]	0.024[d]	13.1[d]	101
F_{30}ZnFbU	<0.002[d]	0.057[d]	0.21[d]	12.9[d]	226
			Monomers		
FbU-β		0.071		13.2	186
F_{15}FbU-β		0.086		12.9	150
ZnU-β	0.033		2.3		70
ZnU′-β	0.035		2.4		69
F_{15}ZnU-β	0.036		1.5		42
FbU		0.12[e]		13.3[e]	111
FbTMP		0.09[e]		13.2[e]	147
FbTPP		0.11[f]		13.0[e]	120
F_{15}FbU′		0.060[e]		13.3[e]	221
F_{20}FbTPP		0.049[d]		11.2[d]	228
ZnU	0.035[e]		2.4		68
ZnTMP	0.039[e]		2.4[e]		62
ZnTPP	0.033[g]		2.0[e]		60
F_{15}ZnU	0.025[e]		1.7[e]		68
F_{15}ZnU′	0.022[e]		1.6[e]		73
F_{20}ZnTPP	0.019[d]		1.4[d]		74

[a] All measurements were made at room temperature. For fluorescence yield and excited-state lifetime measurements, Zn and Fb porphyrins were excited at 550 and 515 nm, respectively. [b] Lifetimes greater than 1 ns (for the β-substituted monomers and dimers studied here) were determined by fluorescence modulation spectroscopy. Lifetimes less than 1 ns were determined by time-resolved absorption spectroscopy. [c] Natural radiative lifetime (inverse of the natural radiative rate) calculated from eq 1. [d] From ref 5. [e] From ref 12. [f] Standard for emission yields for Fb porphyrins from ref 28. [g] Standard for emission from Zn porphyrins from ref 9.

for the corresponding *meso*-tetraarylporphyrins. (2) As is the case for the *meso*-substituted complexes, the presence of pentafluorophenyl groups in the β-substituted complexes blue-shifts (5−7 nm) the bands for the Fb porphyrins but has little or no effect on the band positions for the Zn porphyrins. (3) The Q(0,0)/Q(0,1) intensity ratios are generally reversed for the β- versus *meso*-substituted complexes (Figures 5 and 6). (4) The relative Q-band intensities are generally reversed again in the complexes bearing pentafluorophenyl groups. The combined effect of the last two points is that the Q-band emission ratio for FbU-β is similar to that for F_{15}FbU, and the same is true for F_{15}FbU-β and FbU. The interpretation of the intensity-ratio variations directly parallels that given above for the absorption-intensity ratios concerning the relative energies of the a_{1u} and a_{2u} HOMOs among the complexes.

(3) Fluorescence Quantum Yields and Lifetimes. The quantum yields of the Fb- and Zn-porphyrin emissions for the β-linked dimers and β-substituted monomers are given in Table 1. For comparison, this table also contains the yields obtained previously for the *meso*-substituted analogues. The following points are noteworthy. (1) The extremely low Zn-porphyrin emission yields (<0.002) in ZnFbU-β and F_{30}ZnFbU-β obtained when the Zn-porphyrin is preferentially excited at 550 nm are indicative of a high yield of energy transfer from Zn* to Fb (vide supra). These findings again parallel those for the *meso*-substituted analogues.[3−6] (2) The emission yield of the Fb-porphyrin in ZnFbU-β or F_{30}ZnFbU-β obtained upon exciting the Fb porphyrin near 515 nm is the same as the emission yield of the relevant Fb-porphyrin monomer (FbU-β or F_{15}FbU-β). This finding and parallel results on the lifetimes given below indicate that the presence of the Zn porphyrin in the dimer does not cause any significant quenching of the excited Fb porphyrin (at least in nonpolar solvents such as toluene). (3) The emission characteristics of the corresponding bis-Zn dimers (Zn_2U-β and $F_{30}Zn_2$U-β) are essentially identical with those of the Zn-porphyrin monomers. (4) The presence of pentafluorophenyl groups increases both the Fb-porphyrin and Zn-porphyrin emission yields in the β-substituted complexes by roughly 20%. This effect is opposite that observed for pentafluorophenyl substitution of the *meso*-substituted complexes, wherein the emission yields are reduced by up to about 50% (Table 1).[5,12]

The excited-singlet-state lifetimes of most of the β-substituted compounds were determined via fluorescence techniques (the Zn-porphyrins in the ZnFb dimers were measured by transient absorption spectroscopy (vide infra)). The values are given in Table 1 along with those obtained previously for the *meso*-substituted analogues. In general, for both substitution types, the excited-state lifetimes for the Fb porphyrins are in the range 11.0−13.5 ns and the lifetimes for the Zn porphyrin monomers are in the range 1.5−2.5 ns. Given these ranges and the experimental error, the following points can be made. (1) The excited-state lifetimes are essentially the same in the β- and *meso*-substituted complexes. (2) The Fb* lifetimes (in the dimers and monomers) may be reduced slightly upon introduction of pentafluorophenyl groups. (3) The Zn* lifetimes (in the monomers) are clearly reduced in the complexes with pentafluorophenyl groups.

The emission yields (Φ) and lifetimes (τ) can be combined to obtain the natural radiative rate constant (k_{rad}) via the relation

$$\Phi = k_{rad}\tau \qquad (1)$$

This equation assumes that there are no quenching processes such as energy and electron transfer, which is appropriate for the monomers and the Fb porphyrins in the dimers.[3−6] The results are given in Table 1, which lists the natural radiative lifetime, $(k_{rad})^{-1}$. It can be seen that the presence of pentafluorophenyl groups results in substantially decreased natural radiative lifetimes (increased radiative rates) for the β-substituted complexes. The opposite is true for the *meso*-substituted porphyrins (except for the Zn porphyrin monomers, where little effect is observed). These results qualitatively parallel the trends noted above in the absorption and emission origin-band intensities because k_{rad} also governs the oscillator strengths for the $S_0 \leftrightarrow$ Q-state transitions. The latter in turn is derived, under the four-orbital model, from the relative energies of the a_{1u} and a_{2u} orbitals (vide supra). Thus, the combined fluorescence yields/lifetimes, like the absorption and emission spectral intensities, reflect the mutual effects of β- versus *meso*-substitution and the presence of electron-releasing/-withdrawing substituents on a_{2u}/a_{1u} spacings in the porphyrin constituents of the dimers.

(4) Transient Absorption Spectra. The energy-transfer rate from the photoexcited Zn porphyrin (Zn*) to the ground-state Fb porphyrin subunit in each of the β-linked dimers (ZnFbU-β and F_{30}ZnFbU-β) was assessed using transient absorption spectroscopy. Representative data are shown in Figures 7 and 8. Each of the β-linked dimers was excited using a 120-fs pulse at 550 nm, which predominantly pumps the Zn porphyrin component of each dimer (see Figure 3). Hence, the visible-region absorption difference spectra ($\Delta A = A_{\text{excited state}} - A_{\text{ground state}}$) for ZnFbU-$\beta$ and F_{30}ZnFbU-β observed shortly after excitation are dominated by features characteristic of Zn*. The most notable features are the bleachings of the ground-state absorption bands (troughs in the difference spectra) imbedded on a broad featureless transient absorption that is typical of

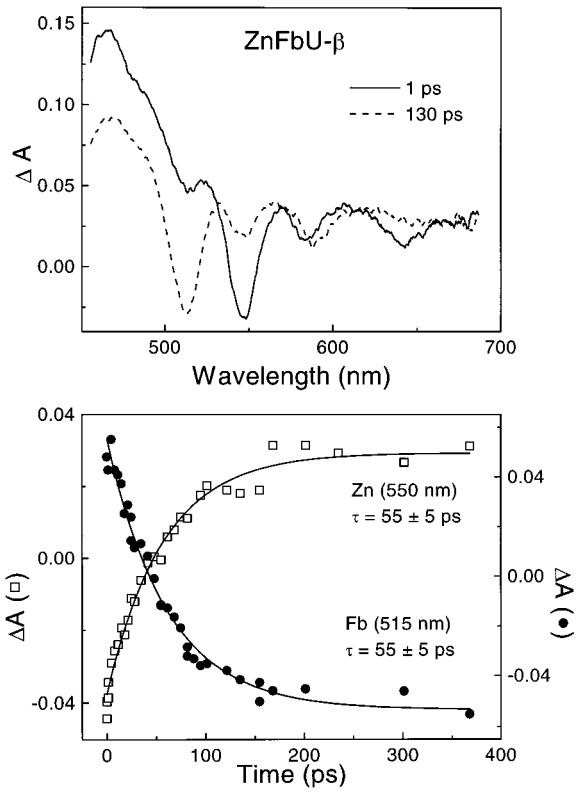

Figure 7. Time-resolved absorption data for ZnFbU-β in toluene at room temperature acquired using a 120 fs 550 nm excitation flash.

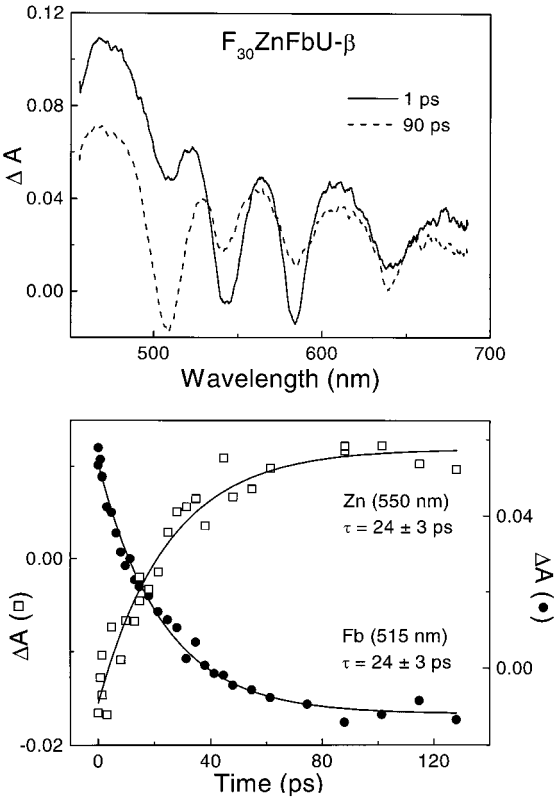

Figure 8. Time-resolved absorption data for F_{30}ZnFbU-β in toluene at room temperature acquired using a 120 fs 550 nm excitation flash.

porphyrin excited states in the visible region.[14] As time proceeds, the spectra for both dimers exhibit a diminution of the signatures of Zn* and the development of spectral characteristics of the photoexcited Fb porphyrin (Fb*), resulting from the Zn*Fb → ZnFb* energy-transfer process. The salient features of the transient absorption data for each complex are described below.

The early-time transient spectra for ZnFbU-β are characterized by bleaching of the Zn-porphyrin Q(1,0) ground-state absorption band near 550 nm together with bleachings of the weaker Q(2,0) and Q(0,0) bands near 510 and 585 nm, respectively (1 ps spectrum in Figure 7). The relative amplitudes of these three features are consistent with (1) the ground-state absorption spectra of reference monomers such as ZnU-β (Figure 3) and (2) the fact that the trough near 585 nm necessarily contains comparable contributions from bleaching of the Zn-porphyrin Q(0,0) ground-state absorption band and from Zn* Q(0,0) stimulated (by the white-light probe pulse) emission.[15] Similarly, the trough near 640 nm in the 1 ps spectrum of ZnFbU-β can be ascribed to Zn* Q(0,1) stimulated emission (Figure 7). The amplitude of the 640 nm feature relative to the ~50% contribution of Q(0,0) stimulated emission to the 585 nm feature at 1 ps is consistent with the ~4/1 amplitude ratio of the corresponding spontaneous-emission bands for ZnU-β (Figure 5C). Collectively, these observations indicate that the 1 ps transient difference spectrum of ZnFbU-β can be assigned essentially exclusively to Zn*.[16]

At increasing times after excitation, the contribution of Zn* to the transient spectra of ZnFbU-β diminishes and the contribution of Fb* increases. Most notably, there is decay of the Zn* 550 nm Q(1,0) bleaching and growth of the 515 nm Fb* Q_y-(1,0) bleaching along with bleaching in the three other Q-bands in the Fb ground-state spectrum (130 ps spectrum in Figure 7). The four Q-region troughs in the 130 ps spectrum are imbedded on a featureless excited-state absorption due to Fb*. The relative amplitudes of these four features are consistent with (1) the amplitude ratios seen in the ground-state absorption spectra of the FbU-β reference monomer (Figure 3B) and (2) the fact that the Q(0,0) feature near 640 nm contains both Fb ground-state bleaching and Fb* stimulated emission. Thus, the spectra at long times (e.g., 130 ps) after excitation of ZnFbU-β are readily assigned to Fb*.

The time evolution of the spectra for ZnFbU-β reflects the Zn* lifetime, which will be shown below to be determined primarily by the energy-transfer process Zn*Fb → ZnFb*. Typical kinetic data are given in Figure 7. The decay of the Q(1,0) bleaching for the Zn porphyrin at 550 nm and the growth of the Q_y(1,0) bleaching for the Fb porphyrin at 515 nm both occur with a time constant of 55 ± 5 ps.

Similar time-resolved absorption measurements were carried out for the pentafluorophenyl-substituted counterpart, F_{30}ZnFbU-β. Representative spectral and kinetic data for this dimer are shown in Figure 8. These data can be evaluated by direct analogy to the description presented above for ZnFbU-β. In particular, the spectrum at 1 ps is dominated by bleaching and stimulated-emission contributions associated with Zn* and the spectrum at 90 ps is assignable to Fb*. However, the time-

(14) Rodriguez, J.; Kirmaier, C.; Holten, D. *J. Am. Chem. Soc.* **1989**, *111*, 6500−6506.

(15) The Zn* Q(0,0) stimulated emission in ZnFbU-β occurs at essentially the same wavelength as the Q(0,0) spontaneous emission observed near 585 nm for ZnU-β (Figure 5C), and this emission in turn is only slightly red-shifted from the Q(0,0) ground-state absorption band (Figure 3C).

(16) There may be a minor contribution from the excited Fb porphyrin (Fb*) in a small fraction of the dimers in which the Fb porphyrin (rather than the Zn porphyrin) was pumped by the 550-nm excitation flash. Note that the quasi-selective excitation of the Zn porphyrin over the Fb porphyrin is enhanced in ZnFbU-β relative to the *meso*-linked analogue ZnFbU.[4,5] This enhancement arises because the amplitude of the 550 nm Q_y(0,0) ground-state absorption band is diminished in the Fb porphyrins in which a β substituent replaces one *meso* substituent (e.g., FbU-β in Figures 1 and 3) relative to the strictly *meso*-substituted complexes (e.g., FbU in Figures 2 and 4).

resolved spectral data for F_{30}ZnFbU-β differ from those for ZnFbU-β in several respects. (1) There are small differences in the amplitude ratios of the features in the transient spectra that follow directly from the corresponding differences in the ground-state absorption and excited-state emission spectra of the pentafluorophenyl-substituted and mesityl-substituted dimers (Figures 3 and 5). (2) There may be a slightly larger contribution of Fb* to the early-time spectrum resulting from photoexcitation of the Fb porphyrin (rather than the Zn porphyrin) in a minor fraction of the dimers.[17] (3) The Zn* lifetime for F_{30}ZnFbU-β is 24 ps. This last result reflects an approximately 2-fold faster rate of energy transfer in the pentafluorophenyl-substituted versus mesityl-substituted dimers, as will be shown in the analysis that follows.

(5) Energy-Transfer Rates and Mechanisms. The transient absorption data, as well as the static and time-resolved fluorescence data, all lead to the assessment that energy transfer from Zn* to the Fb porphyrin in ZnFbU-β and F_{30}ZnFbU-β is a rapid and highly efficient process. This fact can be seen from the following observations. (1) The time constant for the decay of the Zn porphyrin bleaching matches that for the growth of the Fb porphyrin bleaching for both dimers. (2) The Zn* lifetime for each dimer (55 ps for ZnFbU-β and 24 ps for F_{30}ZnFbU-β) is roughly 50-fold shorter than the lifetime for the Zn-porphyrin reference monomer (2.3 ns for ZnU-β and 1.5 ns for F_{15}ZnU-β). (3) The emission yield for the Zn component of each ZnFb dimer is similarly reduced from the values for the corresponding Zn porphyrin reference compound (Table 1).

The rate and yield of Zn*Fb $\rightarrow$ ZnFb* energy transfer for both ZnFbU-β and F_{30}ZnFbU-β can be obtained from either the transient absorption or static emission data. However, the former results give a better assessment, given the predominance of the energy-transfer channel for the Zn* decay in these complexes. The energy-transfer parameters are obtained from

$$1/\tau_D = k_{rad} + k_{isc} + k_{ic} \quad (2)$$

$$1/\tau_{DA} = k_{rad} + k_{isc} + k_{ic} + k_{trans} \quad (3)$$

$$k_{trans} = 1/\tau_{DA} - 1/\tau_D \quad (4)$$

$$\Phi_{trans} = k_{trans}\tau_{DA} = 1 - \tau_{DA}/\tau_D \quad (5)$$

Here, τ_{DA} is the excited-state lifetime of the donor in the presence of the acceptor (i.e., Zn* in the ZnFb dimer), τ_D is the excited-state lifetime of the benchmark Zn-porphyrin monomer, k_{trans} is the measured energy-transfer rate, and Φ_{trans} is the energy-transfer efficiency. These equations assume that, besides energy transfer, there are no pathways for depopulating Zn* in the dimers other than the intrinsic processes (radiative decay (rad), intersystem crossing (isc), internal conversion (ic)) also present in the monomer. Again, the transient absorption and static emission data support this assumption. However, within experimental uncertainty we cannot exclude the possibility of a small amount of electron transfer from the Zn* state.[18]

Table 2 gives the energy-transfer rate constants and yields obtained by application of eqs 2−5 to the excited-state lifetimes.

Table 2. Energy-Transfer and Hole/Electron Hopping Parameters

compd	k_{trans}^{-1} (ps)[a]	Φ_{trans}[a]	k_{hop}^{-1} (μs)[b]
ZnFbU-β	56	0.98	*c*
Zn_2U-β			$\leq$0.05[e]
F_{30}ZnFbU-β	24	0.98	*c*
$F_{30}Zn_2$U-β			*f*
ZnFbU	24[d]	0.99[d]	*c*
Zn_2U			$\leq$0.05[e]
F_{30}ZnFbU	240[d]	0.87[d]	*c*
$F_{30}Zn_2$U			$\geq$2.5[d]

[a] Obtained using the time-resolved optical data and eqs 2−5. [b] Estimated from the 295 K EPR data (see text). [c] No hole/electron hopping occurs in the ZnFb dimers because of the large disparity in oxidation potential of the Zn and Fb constituents.[7,9] [d] From ref 12. [e] From ref 2. [f] The hole/electron hopping rate in $[F_{30}Zn_2U\text{-}\beta]^+$ appears to be in the fast exchange limit (as is the situation for $[Zn_2U\text{-}\beta]^+$) rather than in the slow-exchange limit where $[F_{30}Zn_2U]^+$ resides. However, we are cautious about quantitative assessments from the EPR data because $[F_{30}Zn_2U\text{-}\beta]^+$ could not be prepared quantitatively (see text).

For comparison, Table 2 also contains the results of similar measurements and analyses that we carried out previously on the *meso*-linked dimers ZnFbU and F_{30}ZnFbU.[3−5] The key feature is that the electron-withdrawing effect of the pentafluorophenyl groups increases the excited-state energy-transfer rate in the β-linked dimers, which is exactly opposite that observed for the *meso*-linked dimers.

Our previous studies have shown that excited-state energy transfer in the *meso*-linked arrays is predominantly TB in nature and that through-space (TS) processes make a relatively minor contribution to the overall energy-transfer rate.[3−6] The TS energy-transfer contribution can be evaluated in terms of a Förster mechanism (see Supporting Information). The Förster process is mediated by the donor−acceptor distance and orientation as well as their emission and absorption characteristics (spectral overlap). The similarities in these various properties of the *meso*- versus β-linked dimers dictates that the TS contribution to energy transfer must be qualitatively similar in the two classes of arrays. Explicit calculation of the TS energy-transfer rate for the β-linked dimers (see Supporting Information) confirms that the TS rates are indeed much slower ($\sim$15-fold) than the observed rates, consistent with a dominant TB mechanism.

Following our earlier studies,[3−6] the relative contributions of TS (χ_{TS}) and TB (χ_{TB}) energy transfer to the overall rate can be quantitated using eqs 6−8. The values for the energy-transfer

$$k_{trans} = k_{TB} + k_{TS} \quad (6)$$

$$\chi_{TS} = k_{TS}/k_{trans} \quad (7)$$

$$\chi_{TB} = k_{TB}/k_{trans} \quad (8)$$

parameters of ZnFbU-β and F_{30}ZnFbU-β are summarized in Table 3. For comparison, the values previously determined for the *meso*-linked analogues are also included in Table 3.[3,5] Inspection of Table 3 reveals that the energy-transfer efficiency in both ZnFbU-β and F_{30}ZnFbU-β is extremely high ($\sim$98%) and that the TB contribution accounts for greater than 90% of the observed rate.

C. Physical Properties of the Oxidized Complexes. The oxidized complexes were investigated to gain further insight into the nature of the HOMOs in the β-linked dimers and to assess how linkage at the β-positions modulates ground-state hole/electron transfer.[5,19] These rates are of interest because no independent assessment of the rates of charge transfer is

(17) The simultaneous photoproduction of the long-lived ($\tau \approx 13$ ns) Fb* state in a small fraction of the arrays in which Fb* (and not Zn*) is photopumped does not affect the Zn* lifetime or energy-transfer rate in the (predominant) fraction in which Zn* is photoproduced.[4,6,12]

(18) We have excluded the possibility of a significant amount (<10%) of photoinduced charge transfer in other dimers in this series, including ZnFbU and F_{30}ZnFbU.[3−7] For example, solvents of differing polarity have essentially no effect on the Zn* lifetime in the latter systems. Given all available information, there is no reason to expect that charge transfer is significantly enhanced in ZnFbU-β and F_{30}ZnFbU-β.

(19) Seth, J.; Palaniappan, V.; Johnson, T. E.; Prathapan, S.; Lindsey, J. S.; Bocian, D. F. *J. Am. Chem. Soc.* **1994**, *116*, 10578−10592.

Table 3. Through-Bond and Through-Space Energy-Transfer Rates and Efficiencies for Various ZnFb Dimers[a]

compd	Φ_{trans}[b]	k_{trans}^{-1} (ps)[b]	k_{TS}^{-1} (ps)[c]	k_{TB}^{-1} (ps)[d]	χ_{TS}[e]	χ_{TB}[f]
ZnFbU	0.99	24	745	25	0.04	0.96
F_{30}ZnFbU	0.87	240	1326	292	0.18	0.82
ZnFbU-β	0.98	56	833	60	0.07	0.93
F_{30}ZnFbU-β	0.98	24	382	30	0.06	0.94

[a] All data were obtained in toluene at room temperature. The parameters for the *meso*-linked dimers were taken from refs 5 and 12. [b] Obtained using eqs 2−5 and the lifetime data in Table 1. [c] Obtained from the Förster energy transfer calculation using $R = 20$ Å and $\kappa^2 = 1.125$ for the *meso*-linked dimers, and $R = 20.8$ Å and $\kappa^2 = 1.25$ for the β-linked dimers (see the Supporting Information). [d] Obtained using eq 6. [e] Obtained using eq 7. [f] Obtained using eq 8.

Table 4. Half-Wave Potentials[a] for Oxidation of the Zn Porphyrins

complex	$E_{1/2}(1)$	$E_{1/2}(2)$
ZnU-β	0.62	0.89
Zn_2U-β[b]	0.62	0.89
F_{15}ZnU-β	1.05	1.27
$F_{30}Zn_2$U-β[b]	1.05	1.27

[a] Obtained in CH_2Cl_2 containing 0.1 M TBAH. $E_{1/2}$ values are given vs Ag/Ag^+; $E_{1/2}$ of $FeCp_2/FeCp_2^+ = 0.22$ V (scan rate 0.1 V/s). Values are ±0.01 V. [b] The redox waves of the two Zn porphyrins are not resolved by cyclic voltammetry.

available for the neutral arrays. Although the hole/electron hopping rates in the ground electronic states of the cations are not expected to be equal to the charge-transfer rates in the excited states of the neutrals, they at least provide some measure of the factors that control this type of process.

(1) Electrochemistry. The $E_{1/2}$ values for oxidation of the Zn porphyrins in the β-linked dimers and the β-substituted monomeric reference compounds are summarized in Table 4. The two $E_{1/2}$ values listed in the table correspond to the first and second oxidations of the porphyrin ring.[20,21] In general, the redox potentials of the β-linked dimers and β-substituted monomers closely resemble those of the analogous *meso*-diarylethyne complexes.[2,5] The redox properties of the Zn constituents in these dimers are essentially identical with those of monomeric Zn porphyrins, indicating that the ground-state interactions between the porphyrin constituents of the dimers are relatively weak. The ground-state interaction between the π-systems of the diphenylethyne linker and the porphyrin rings is also quite weak.[2,5] Accordingly, the replacement of the *meso*-diphenylethyne linker with the β-diphenylethyne linker does not result in any clearly detectable change in the magnitude of the ground-state interaction between the porphyrins in the dimers.

The only notable difference in the redox characteristics of the β-linked versus *meso*-linked dimers was in the behavior of $F_{30}Zn_2$U-β under bulk electrolysis conditions. In particular, bulk electrolysis of $F_{30}Zn_2$U-β failed to generate either the mono- or dicationic species in quantitative amounts, as judged by spectroscopic studies after the electrolysis. The reason for this is not certain, particularly considering that both the mono- and dications of the monomeric reference compound F_{15}ZnU-β could be quantitatively obtained and were stable for extended periods (hours). Regardless, the inability to quantitatively generate $[F_{30}Zn_2U\text{-}\beta]^+$ potentially compromises the interpretation of the EPR data for this complex (vide infra).

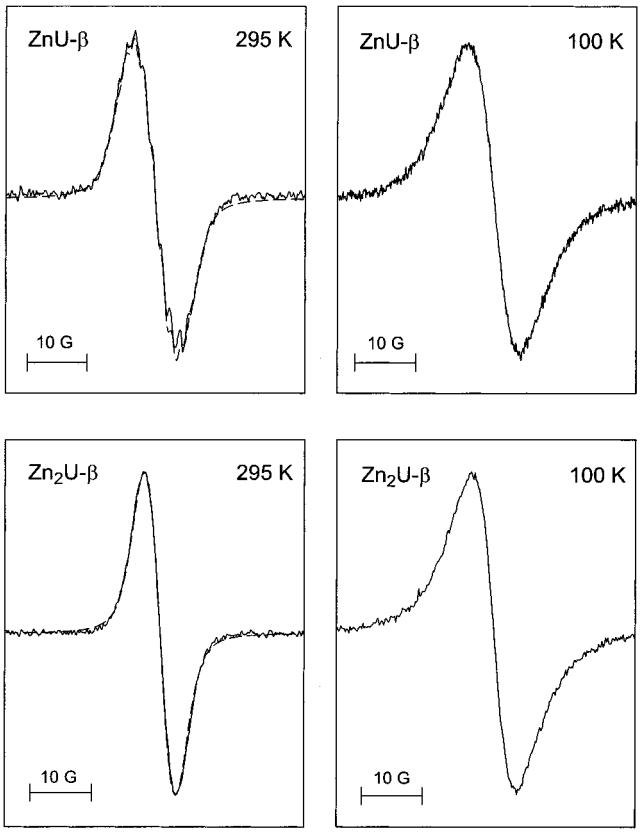

Figure 9. EPR spectra of $[ZnU\text{-}\beta]^+$ and $[Zn_2U\text{-}\beta]^+$ at 295 and 100 K. The additional dotted traces shown at 295 K are simulated spectra.

2. Absorption Spectra. The UV−vis absorption characteristics of the mono- and dications of the β-linked dimers and β-substituted monomeric reference compounds (not shown) are typical of those of other porphyrin π-cation radicals, namely weaker, blue-shifted B-bands (relative to the neutral complexes) and very weak, broad bands in the visible and near-infrared regions.[20] The absorption spectra of the oxidized complexes appear to be a superposition of the spectra of the neutral and cationic species of the different porphyrin units. This observation, like the results of the electrochemical studies,[22−25] is consistent with weak interactions between the constituent porphyrins.

3. EPR Spectra. The EPR spectra of the one-electron-oxidation products of ZnU-β and Zn_2U-β in CH_2Cl_2 at 295 and 100 K are shown in Figure 9. The spectra of the one-electron-oxidation product of F_{15}ZnU-β obtained under the same conditions are shown in Figure 10. The spectra for oxidized $F_{30}Zn_2$U-β are not shown because the nonquantitative formation of this species renders the data suspect. The EPR spectra of all of the cations were examined as a function of sample concentration. No changes in hyperfine splittings or line shape were observed for the concentrations used for the EPR studies (≤0.05 mM). Consequently, the differences observed

(20) Felton, R. H. In *The Porphyrins*; Dolphin, D., Ed.; Academic Press: New York, 1978; Vol. V, pp 53−126.
(21) Davis, D. G. In *The Porphyrins*; Dolphin, D., Ed.; Academic Press: New York, 1978; Vol. V, pp 127−152.
(22) Heath, G. A.; Yellowlees, L. J.; Braterman, P. S. *J. Chem. Soc., Chem. Commun.* **1981**, 287−289.
(23) Elliot, C. M.; Hershenhart, E. *J. Am. Chem. Soc.* **1982**, *104*, 7519−7526.
(24) Edwards, W. D.; Zerner, M. C. *Can. J. Chem.* **1985**, *63*, 1763−1772.
(25) (a) Angel, S. M.; DeArmond, M. K.; Donohoe, R. J.; Wertz, D. W. *J. Phys. Chem.* **1985**, *89*, 282−285. (b) Donohoe, R. J.; Tait, C. D.; DeArmond, M. K.; Wertz, D. W. *Spectrochim. Acta* **1986**, *42A*, 233−240. (c) Tait, C. D.; MacQueen, D. B.; Donohoe, R. J.; DeArmond, M. K.; Hanck, K. W.; Wertz, D. W. *J. Phys. Chem.* **1986**, *90*, 1766−1771. (d) Donohoe, R. R.; Tait, C. D.; DeArmond, M. K.; Wertz, D. W. *J. Phys. Chem.* **1986**, *90*, 3923−3926. (e) Donohoe, R. J.; Tait, C. D.; DeArmond, M. K.; Wertz, D. W. *J. Phys. Chem.* **1986**, *90*, 3927−3930.

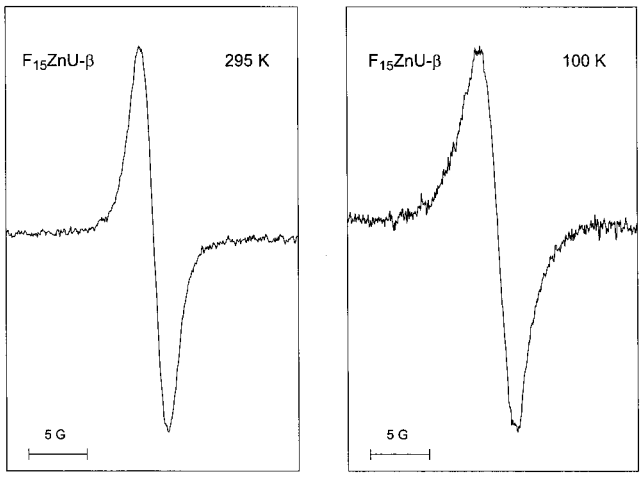

Figure 10. EPR spectra of $[F_{15}ZnU\text{-}\beta]^+$ at 295 and 100 K.

in the spectral features of the various complexes are intrinsic and cannot be ascribed to intermolecular interactions.

Examination of the EPR signatures of the cations of the various β-substituted monomeric reference compounds and β-linked dimers reveals the following features.

(1) The liquid- and frozen-solution EPR spectra of $[ZnU\text{-}\beta]^+$ are qualitatively similar to those of the analogous spectra of $[ZnTMP]^+$ (TMP is *meso*-tetramesitylporphyrin) and monomeric analogues that contain a *meso*-ethynylphenyl substituent (e.g., $[ZnU]^+$).[2,19] In particular, the liquid-solution EPR signal of $[ZnU\text{-}\beta]^+$ exhibits a poorly resolved nine-line hyperfine pattern due to interaction of the unpaired electron with the four pyrrole ^{14}N nuclei (Figure 9, upper left panel). This hyperfine pattern is characteristic of a $^2A_{2u}$ porphyrin π-cation radical.[26] Quantitative fitting of the EPR line shape (dashed line superimposed on the spectrum) reveals that the hyperfine coupling constant has a value of $a(^{14}N) \approx 1.42$ G. This coupling constant is comparable to that observed for the ZnTMP cation[2,19] (and the oxidized tetraphenyl analogue ZnTPP[26]). The simulations of the EPR spectra of $[ZnU\text{-}\beta]^+$ also indicate that the line shape cannot be accurately fit without the additional inclusion of hyperfine coupling to a single ^1H nucleus with $a(^1H) \approx 3.4$ G. This feature of the spectra is consistent with the β-substituted porphyrin architecture, which is characterized by a single *meso* hydrogen (Figure 2). The hyperfine coupling to this hydrogen would be expected to be significant in a $^2A_{2u}$ porphyrin π-cation radical because of the substantial spin density at the *meso*-carbon atom.[19]

The liquid-solution EPR signal of $[Zn_2U\text{-}\beta]^+$ exhibits a much narrower line than $[ZnU\text{-}\beta]^+$ with no resolved hyperfine structure (Figure 9, lower left panel). Simulations of the EPR spectrum of $[Zn_2U\text{-}\beta]^+$ indicate that the line shape is well accounted for by halving the ^{14}N and $^1H_{meso}$ hyperfine couplings and doubling the number of interacting nuclei (while holding the line width constant). This behavior indicates that the hole/electron of $[Zn_2U\text{-}\beta]^+$ is completely delocalized on the EPR time scale, as is also the case for the *meso*-linked diphenylethyne dimer $[Zn_2U]^+$.[2] This time scale is determined by the magnitude of the ^{14}N hyperfine coupling, which is $\sim$4.2 MHz.[2,26] Thus, the hole/electron hopping rate is $\geq(0.05\ \mu s)^{-1}$. When the solution is frozen, the EPR signal of $[Zn_2U\text{-}\beta]^+$ broadens and is essentially identical with the signal observed for $[ZnU\text{-}\beta]^+$ in frozen solution (Figure 9, right panels). This behavior indicates that the hole/electron becomes localized (on the EPR time scale) on one of the Zn constituents of $[Zn_2U\text{-}\beta]^+$ ($\leq(1\ \mu s)^{-1}$). This behavior again parallels that observed for $[Zn_2U]^+$, in which the hole/electron hops rapidly in liquid solution but becomes localized in frozen solution.[2]

(2) The liquid- and frozen-solution EPR spectra of $[F_{15}ZnU\text{-}\beta]^+$ are very similar to those of the analogous spectra of the *meso*-diphenylethyne-substituted monomer $[F_{15}ZnU']^+$.[5] In particular, the liquid-solution EPR signal of $[F_{15}ZnU\text{-}\beta]^+$ is relatively sharp (peak-to-peak width $\sim$5 G) and exhibits no resolved hyperfine splittings (Figure 10). The ^{14}N hyperfine splittings are absent for $[F_{15}ZnU\text{-}\beta]^+$ because the strongly electron-withdrawing pentafluorophenyl groups at the nonlinking *meso* positions energetically stabilize the a_{2u} molecular orbital,[10,27] resulting in a ground state that is solely, or mostly, $^2A_{1u}$-like in character.[5] The a_{1u} molecular orbital, which contains the unpaired electron in these latter types of radicals, has appreciable electron density on the β-pyrrole carbon atoms, but nodal planes through the pyrrole nitrogen atoms (and *meso*-carbon atoms).[9,10] The liquid- and frozen-solution EPR signals observed for $[F_{30}Zn_2U\text{-}\beta]^+$ are also very narrow (not shown), with peak-to-peak widths somewhat smaller than those of $[F_{15}ZnU\text{-}\beta]^+$. The relatively narrow liquid-solution EPR signal observed for $[F_{30}Zn_2U\text{-}\beta]^+$ is qualitatively consistent with rapid hole/electron hopping in this dimer. The observation that the hole/electron hopping rate for $[F_{30}Zn_2U\text{-}\beta]^+$ is in the fast-exchange limit suggests that this rate is at the very least comparable to that for $[Zn_2U\text{-}\beta]^+$, which is also in the fast-exchange limit. Regardless, the hole/electron hopping rate for $[F_{30}Zn_2U\text{-}\beta]^+$ is clearly not in the slow exchange limit where $[F_{30}Zn_2U]^+$ resides. However, we are cautious about giving a more quantitative assessment of the hole/electron hopping characteristics of $[F_{30}Zn_2U\text{-}\beta]^+$ from the EPR data because this species could not be prepared quantitatively.

III. Discussion

To rationally design molecular architectures for use in nanoscale photonic materials, it is essential to have a fundamental understanding of the relationship between the electronic structure of the active chromophores and how the linking element modulates the interchromophore electronic communication. Our previous studies have shown that a *meso*-diarylethyne linker supports ultrafast, highly efficient excited-state energy transfer between the porphyrin constituents and that this process is primarily TB in nature.[3−6] The *meso*-diarylethyne linker also supports robust ground-state hole/electron transfer in π-cation radical species.[2,5,6,19] The results presented herein on the new β-linked architectures indicate that altering the site of attachment of the diarylethyne linker does not change the basic energy-/electron-transfer characteristics of the multiporphyrin arrays. Thus, the diarylethyne linker is a viable synthetic construct for a broad class of molecular architectures. The key observation from the present study is that the addition of strongly electron-withdrawing pentafluorophenyl groups to the nonlinking porphyrin constituents *enhances* electronic communication in a β-diarylethyne-linked array, whereas these same substituents *attenuate* electronic communication in a *meso*-diarylethyne-linked array. Thus, the studies of the β-linked dimers in conjunction with our previous work on the *meso*-linked arrays explicitly demonstrate how the detailed characteristics of the electronic structure of the porphyrinic chromophore can be used in concert with the connectivity of the diphenylethyne linker to fine-tune the electronic communication in multiporphyrin arrays.

(26) Fajer, J.; Davis, M. S. In *The Porphyrins*; Dolphin, D., Ed.; Academic Press: New York, 1979; Vol. IV, pp 197−256.

(27) Ghosh, A. *J. Am. Chem. Soc.* **1995**, *117*, 4691−4699.

(28) Seybold, P. G.; Gouterman, M. *J. Mol. Spectrosc.* **1969**, *31*, 1−13.

More importantly, the collected studies demonstrate that the electronic factors associated with orbital tuning and the linking site play a central role in mediating electronic communication, in addition to the more commonly considered factors of distance, orientation, and energetics.

In the sections below, we first discuss the general attributes of the interplay between porphyrin electronic structure and linker connectivity. We then examine in more detail the factors that differentiate the electronic communication in β- versus *meso*-linked multiporphyrin arrays. Finally, we consider the implications for the design of molecular photonic devices.

A. General Effects of Porphyrin Electronic Structure and Linker Connectivity on Electronic Communication. The electron density at the sites of linker attachment to the donor and acceptor macrocycles strongly modulates the TB interporphyrin electronic coupling. Several factors must be considered in this regard, including the following: (1) the inherent electron-density distributions of the frontier molecular orbitals that contribute to the wave functions for the relevant electronic states, (2) the manner in which relative and absolute π-electron densities on the various atoms in the porphyrin macrocycle are affected by the electron-withdrawing/-releasing character and positions of the nonlinking peripheral substituents, and (3) the site of linker attachment relative to the electron density distributions in the macrocycle.

Consider first only the two top-filled porphyrin orbitals (a_{1u}, a_{2u}). The a_{1u} versus a_{2u} orbitals place substantially different amounts of electron density at the β-pyrrole versus *meso* positions (see Figure 1). The energy spacing/ordering of these two orbitals and the distribution of electron density throughout the porphyrin can be substantially altered by the positions and electron-withdrawing/-releasing character of the nonlinking peripheral substituents. The ordering and energetic spacing of the a_{1u} and a_{2u} orbitals in a given porphyrin dictates which of the two will make the greatest relative contribution to the appropriate ground- and excited-state wave functions and thereby to the linker-mediated interporphyrin electronic coupling. The combined optical and EPR data presented in this and previous work[2−6,12] for a host of relevant monomeric building blocks indicate that although there are differences in orbital energies between the β- and *meso*-substituted porphyrins, regardless of the position of linker attachment, the porphyrins bearing mesityl rings at the three nonlinking *meso* positions have an a_{2u} HOMO, whereas the corresponding pentafluorophenyl-substituted porphyrins have an a_{1u} HOMO. The overall similarity in orbital-energy relationships for the two porphyrin classes results from the fact that positioning the linker at the β versus *meso* site (i.e., replacing one of four *meso*-aryl groups with a hydrogen and one of eight β-hydrogens with a diphenylethyne linker) is a minor perturbation that does not substantially alter the overall electronic structure of the macrocycle.

The above considerations provide a qualitative framework for understanding the reversal in the effects of (electron-releasing) mesityl versus (electron-withdrawing) pentafluorophenyl groups at the nonlinking positions on electronic communication in the *meso*- versus β-linked dimers. In particular, the slower excited-state energy transfer observed for F_{30}-ZnFbU versus ZnFbU (and slower ground-state hole/electron hopping in $[F_{30}Zn_2U]^+$ versus in $[Zn_2U]^+$) is dictated by the change in the characteristics of the electronic wave functions that mediate the processes. The change in wave function in turn arises largely from the switch in the HOMO from a_{2u} to a_{1u}. The enhanced contribution of the a_{1u} orbitals to the relevant wave functions in the pentafluorophenyl-substituted dimers linked at the *meso* sites necessarily attenuates the electronic coupling owing to the absence of electron density at this position in the a_{1u} orbital (Figure 1). In the β-linked dimers, the incorporation of these same pentafluorophenyl groups also reverses the energy ordering of the a_{1u} and a_{2u} orbitals and thereby enhances a_{1u}-orbital contribution to the salient wave functions. In this case, electronic communication in F_{30}ZnFbU-β is enhanced relative to that in the ZnFbU-β (the same is true in monocations of the bis-Zn complexes) because the a_{1u} orbital has larger β-pyrrole electron density than does the a_{2u} orbital.[9,10] (Note that higher level molecular orbital calculations predict that the a_{2u} orbital has a small amount of electron density at the β-carbons; the density is zero only in Huckel calculations.) These considerations of the HOMO characteristics provide a straightforward qualitative picture of how orbital tuning and linker site together modulate interporphyrin electronic communication in the multiporphyrin arrays. Various other factors come into play to determine the detailed aspects of the electronic communication in the *meso*- versus β-linked arrays, as are discussed in the next section.

B. Additional Factors Affecting the Magnitudes of Electronic Communication in the β- versus *meso*-Linked Arrays. The effects of electron-withdrawing pentafluorophenyl groups on electronic communication in the *meso*-linked dimers are much larger than in the β-linked dimers. In particular, the presence of pentafluorophenyl groups results in a 10-fold attenuation in the energy-transfer rate for the former class of dimers compared with only a 2.3-fold enhancement in the latter class (Table 3). In addition, the energy-transfer rates are comparable for ZnFbU and F_{30}ZnFbU-β, for which the HOMO and site of linker attachment work in concert to enhance electronic communication. In contrast, the energy-transfer rates are quite different for F_{30}ZnFbU versus ZnFbU-β (4.4-fold slower in the former), for which the HOMO and site of linker attachment have opposite effects on electronic communication. Similar effects are manifested in the hole/electron hopping characteristics of the bis-Zn analogues of the two sets of dimers. A number of factors bear on the interpretation of these data.

(1) The positions of the peripheral electron-withdrawing/-releasing substituents cause changes in both the relative and absolute electron densities throughout the macrocycle. The nonlinking aryl substituents are positioned at *meso* carbons and hence will exert their electronic effects predominantly on the a_{2u} orbital rather than the a_{1u} orbital, with different consequences for the *meso*-linked or β-linked dimers. In the *meso*-linked dimers, the electron density at the *meso* carbon of the linker will be strongly influenced by the three nonlinking groups, which also are at *meso* sites (i.e., all are at positions which the a_{2u} orbital has considerable density). In the β-linked dimers, the three nonlinking *meso* groups will have less of an effect on the density at the site of the β-linker because the latter is positioned where the a_{1u} orbital rather than the a_{2u} orbital has substantial density. Accordingly, changes in the electronic properties of the nonlinking *meso* substituents are expected to have proportionately larger effect on the *meso*-linked versus β-linked dimers.

(2) The LUMO characteristics also contribute to interporphyrin electronic communication, perhaps by differing degrees for the β- versus *meso*-linked dimers. The e_{gx} and e_{gy} orbitals of metalloporphyrins have the same electron density at the *meso* sites, and the analogue orbitals of Fb porphyrins have comparable densities at these positions.[9,10] Accordingly, the relative energies of these two orbitals are not expected to alter the electronic communication in the *meso*-linked arrays (although

the absolute electron densities of the LUMOs will change with the electron-withdrawing/-releasing effects of the peripheral substituents). For a β-linked dimer, however, only one of the orbitals has electron density at that site even in metalloporphyrins because the linker lowers the symmetry below D_{4h} (*x* and *y* equivalent). The situation is more complex in a Fb porphyrin acceptor because of the presence of the NH−NH axis (which also lowers the symmetry) and its position with respect to the linker site. Accordingly, one of the two potential LUMOs will contribute more to electronic communication than the other. The magnitude of the contribution will depend on the detailed substitution pattern of the porphyrin constituents of the array.

(3) The degree of torsional freedom of the diphenylethyne linker may differ in the β-linked dimers versus *meso*-linked dimers, thereby altering electronic communication. In this regard, we have previously shown that steric hindrance which suppresses rotation of the linker toward coplanarity with the porphyrin can decrease the rate of excited-state energy transfer by up to 3.5-fold.[2,3,19] In the *meso*-linked dimers, the two flanking β-pyrrole hydrogens are pointed toward the phenylene group of the linker, while in the β-linked dimers, the one *meso* hydrogen is pointed toward the phenylene group of the linker while the flanking β-pyrrolic hydrogen is pointed away from the linker. Thus, steric constraints on torsional mobility should be smaller in the β-linked dimers, thereby enhancing TB communication.

(4) The a_{2u} orbital has lobes on the four *meso* carbons and four nitrogen atoms, whereas the a_{1u} orbital has lobes on 16 carbons, eight of which are at the β-positions. The more extensive delocalization of the a_{1u} orbital results in less electron density at each β-carbon compared with that at each *meso* carbon in the a_{2u} orbital. The greater electron-density delocalization in the a_{1u} orbital should give diminished electronic communication when the a_{1u} orbital is the HOMO compared with the a_{2u} HOMO for a given site of linker substitution.

(5) The diphenylethyne linker is electron releasing (comparable to a phenyl group), and when placed at the β versus *meso* position is expected to stabilize the a_{1u} versus a_{2u} orbital. This effect would enhance electronic communication in β-linked arrays with an a_{1u} HOMO.

Finally, we emphasize that these five factors exert relatively minor influences on the electronic communication in the diarylethyne-linked arrays. The reversal of the a_{2u}/a_{1u} orbitals and the concomitant change in the nature of the ground- and excited-electronic-state wave functions is the dominant contribution to the observed reversal in energy-transfer (electron/hole hopping) rates in the β- versus *meso*-linked dimers with mesityl versus pentafluorophenyl substituents.

C. Implications for the Design of Molecular Devices. The fact that electronic communication in the multiporphyrin arrays depends on both orbital characteristics (ordering, spacing, and electron-density distributions) and site of linker connection impinges directly on design considerations for the incorporation of porphyrins into molecular devices. The rate of energy transfer decreases in the following order: *meso*-linker and a_{2u} HOMO (ZnFbU) $\approx$ β-linker and a_{1u} HOMO (F_{30}ZnFbU-β) > β-linker and a_{2u} HOMO (ZnFbU-β) > *meso*-linker and a_{1u} HOMO (F_{30}-ZnFbU). These results have the following implications. (1) The nature of the HOMO must be considered at the design stage of selecting the overall molecular architecture. If the objective is to enhance electronic communication and the HOMO is an a_{2u} orbital, connection should be made at the *meso* position. For the a_{1u} HOMO, connection should be made at the β position. If the objective is to connect pigments but to suppress communication, then the opposite sites of attachment (at positions where the frontier orbitals exhibit nodes rather than lobes) should be employed. (2) The methods of tuning the HOMO include the choice of electron-withdrawing/-releasing nonlinking groups and how these groups are positioned with respect to the linker site (taking into consideration the electron density distribution in the HOMO). On the basis of a recent study of a large number of monomeric porphyrins with various halogenated aryl groups, we have elucidated how factors such as orbital ordering/spacing, excited-state lifetimes, and redox properties can be tuned with exquisite precision.[12] This library of porphyrins provides considerable leeway for selecting building blocks with the desired properties for performing specific functions in a porphyrin-based molecular photonic device. (3) The electronic effects of the linker must be considered in any rational design strategy. While the linker is primarily viewed as a transmission element in electronic communication, it is not necessarily innocent in altering the orbital properties of the attached pigments.

We anticipate that the effects of orbital tuning and position of connection are quite general for electronic communication processes in covalently linked cyclic polyenes (and other classes of molecules). Other types of processes (besides excited-state energy transfer and ground-state hole/electron hopping) that are expected to depend on the detailed aspects of the molecular design include both photoinduced and thermal electron-transfer reactions. Finally, we note the observation that a reversal in orbital ordering can substantially alter the magnitude of electronic coupling has the potential for permitting the design of a variety of molecular devices.

Acknowledgment. This work was supported by the NSF (Grant No. CHE-9707995 to D.F.B., D.H., and J.S.L.). Support for D.K. was provided by the Creative Research Initiatives of the Ministry of Science and Technology of Korea.

Supporting Information Available: Text giving a complete Experimental Section and a description of the Forster through-space energy transfer calculation and tables of the optical absorption and emission spectral data (PDF). This material is available free of charge via the Internet at http://pubs.acs.org.

JA9842060